Supplementary Information

NOS and SONOS redox switches in proteins

Fabian Rabe von Pappenheim [1,2] , Marie Wensien [1,2] , Jin Ye [3], Jon Uranga [3], Lisa-Marie Funk [1,2], Ricardo A. Mata [3], & Kai Tittmann [1,2] *

[1] Department of Molecular Enzymology, Göttingen Center of Molecular Biosciences, Georg-August University Göttingen, Julia-Lermontowa-Weg 3, D-37077 Göttingen, Germany

[2] Department of Structural Dynamics, Max-Planck-Institute for Biophysical Chemistry, Am Fassberg 11, D-37077 Göttingen, Germany

[3] Institute of Physical Chemistry, Georg-August University Göttingen, Tammannstraße 6, D-37077 Göttingen, Germany

* To whom correspondence shall be addressed: ktittma@gwdg.de (K.T.)

Supplementary Figures

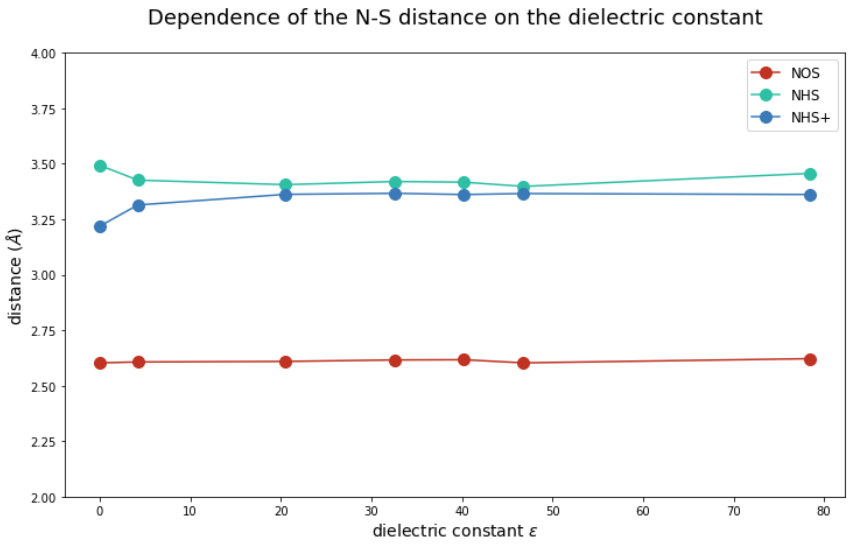

SI Fig. 1. Dependence of the N-S distance on the dielectric constant for the three model situations of Lys-Cys binding. The calculations were carried out for a single sampled conformer at the B3LYP-D3(BJ)/def2-SVP level of theory applying different dielectric constants with the use of the SMD module.

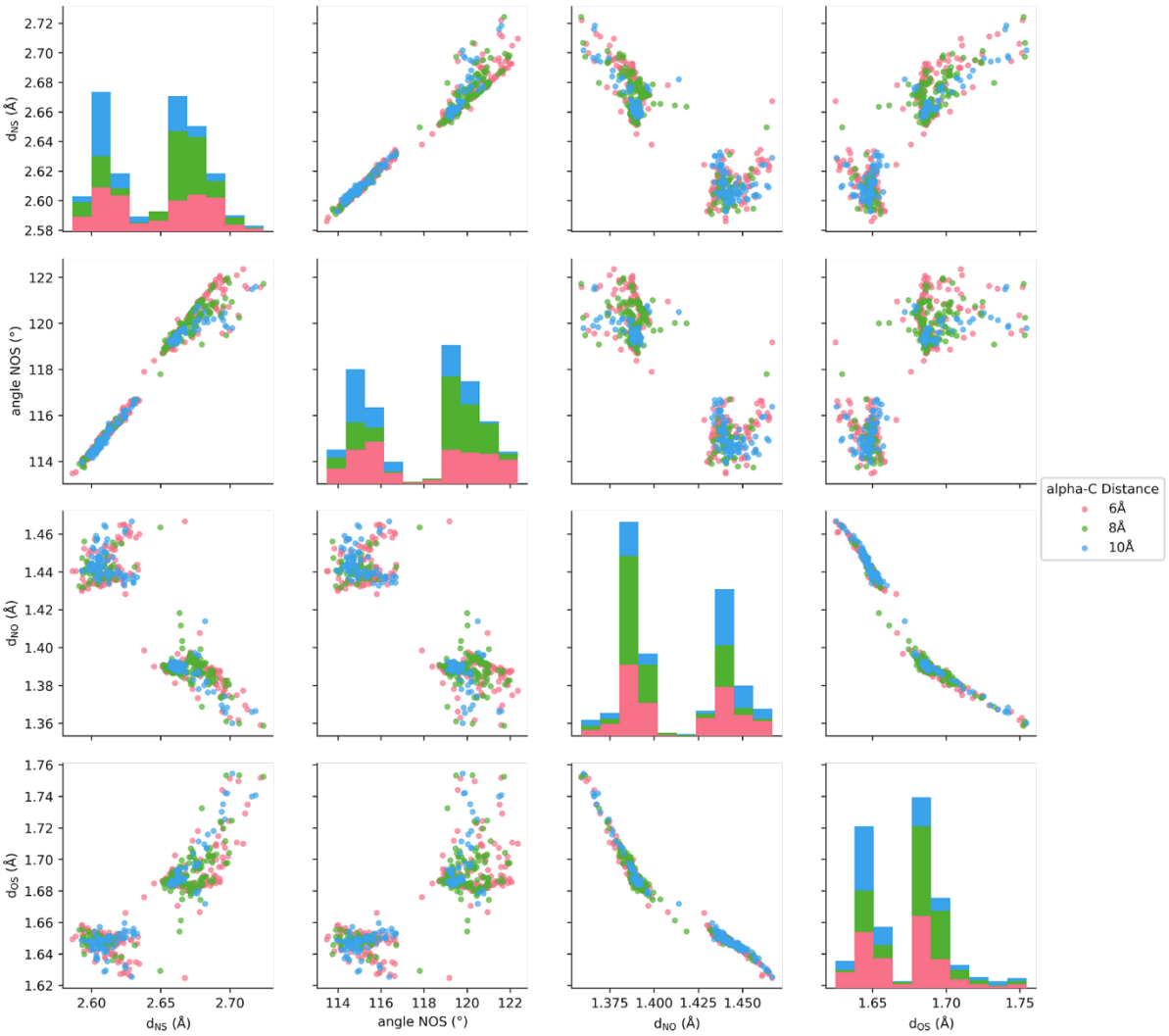

SI Fig. 2. Geometric properties of NOS bridges. Pair plots for four selected structural variables of the NOS bond: N-S distance (dNS), NOS angle (Angle N-O-S), N-O distance (dNO) and O-S distance (dOS). The data used corresponds to the larger set of structures obtained with the def2-SVP basis set (the same as panels a) and b. Several variables correlate strongly. The bimodal distribution of the N-S distances is due to steric constraints between the sulfur atom and the lysine chain, with an interplay between the N-O and the O-S bond distances. The N-O-S angle, as it should be expected, strongly correlates with the N-S distance. The results are largely independent of the distance between the α-carbons of the two chains.

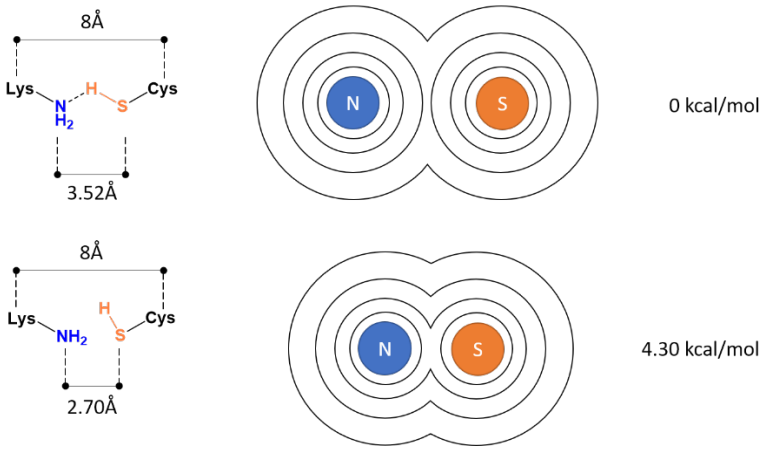

SI Fig. 3. Energy penalty for the constrained N-S-distance of 2.7 Å in NHS (H-bond interaction). Top: electronic energy of the lowest conformer of NHS without the constraint. Bottom: lowest energy conformer of NHS with a constrained N-S distance of 2.7 Å. The electronic energy of the non-constrained conformer is taken as reference.

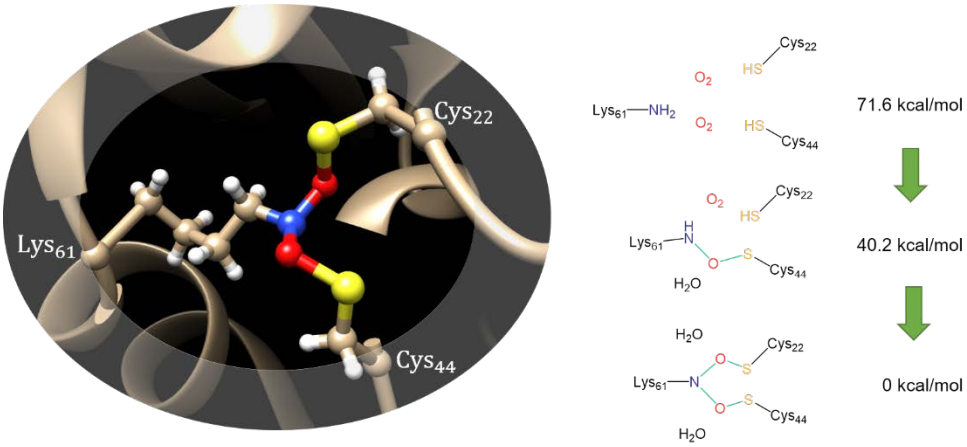

SI Fig. 4. Summary of the thermochemistry in SONOS bond formation using a cluster model of the COVID-19 main protease SONOS site. The calculations were based on the reduced cluster from COVID-19 main protease (PDB code: 7JR4, rebuilt without covalent NOS or SONOS bridge), a structure including only the Cys22, Cys44 and Lys61 residues and truncating the α-carbons (as terminal methyl groups) was taken for the calculation. The educt contained additionally two oxygen molecules, which were turned into the two NOS linkages and water molecules via two steps. The structures were optimised using B3LYP-D3(BJ)/def2-SVPD to obtain the free energy corrections under standard state conditions (T=298.15 K). The electronic energies were refined using B3LYP-D3(BJ)/def2-TZVPD. Calculations at both levels were carried out with the Gaussian16-A.03 program package under the application of the SMD solvation model (water as solvent). The most thermodynamically stable structure (the SONOS linked cluster) was taken as reference for the energies.

Supplementary Tables

SI Table 1. X-ray crystallographic data collection and refinement statistics.

	*Ng*TAL E93Q	*Ng*TAL wt 0.5 MGy	*Ng*TAL wt 5.0 MGy	*Ng*TAL wt 10.0 MGy
	7OEY	7ODO	7ODP	7ODQ
Data collection				
Space group	C 1 2 1	P 21 21 21	P 21 21 21	P 21 21 21
Cell dimensions				
a,b,c (Å)	172.4 55.04 84.37	42.14 82.78 89.36	42.17 82.82 89.4	42.2 82.85 89.42
α, β, γ (°)	90 108.7 90	90 90 90	90 90 90	90 90 90
Resolution (Å)	38.44 - 1.35 (1.398 - 1.35)*	37.55 - 1.40 (1.45 - 1.40)	38.14 - 1.40 (1.45 - 1.40)	37.6 - 1.40 (1.45 - 1.40)
R_{meas}	0.065 (0.865)	0.090 (1.13)	0.099(1.572)	0.112 (2.416)
$CC_{1/2}$	0.998 (0.856)	0.999 (0.856)	0.999 (0.75)	0.999 (0.568)
I/σI	12.67 (1.98)	17.92 (2.41)	16.10 (1.72)	13.85 (1.08)
Completeness (%)	97.80 (97.94)	99.16 (98.07)	99.11 (97.97)	99.08 (97.93)
Multiplicity	4.6 (4.7)	13.4 (13.4)	13.4 (13.4)	13.5 (13.4)
Refinement				
Reflections used in refinement	160763 (16009)	61847 (6047)	61901 (6040)	61970 (6042)
R_{work}/R_{free}	13.7/16.2	13.9/16.2	14.2/16.6	14.8/17.2
Number of non-hydrogen atoms				
macromolecules	5845	2936	2936	2936
ligands	35	13	13	13
solvent	982	434	434	434
Average B-factor				
macromolecules	22.11	17.43	18.91	20.61
ligands	39.37	22.08	24.75	28.94
solvent	35.06	29.25	31.63	33.85
R.m.s deviations				
RMS(bonds)	0.012	0.006	0.006	0.007
RMS(angles)	1.19	0.93	0.97	1.01

* Values in parentheses are for the highest-resolution shell.

SI Table 2. Steady-state kinetic analysis of *Ng*TAL wild-type and variant Glu93Gln under oxidizing (w/o DTT) and reducing (w/ 1 mM DTT) conditions.

Transaldolase		k_{cat} [s^{-1}]	K_M [mM]	k_{cat}/K_M [s^{-1} mM^{-1}]	DTT
N. gonorrhoeae					
wt ox	steady-state basal	0.63 ± 0.02 (0.29 ± 0.01) [a]	9.98 ± 1.28 (9.36 ± 1.33) [a]	0.06 (0.03)	-
wt red	steady-state	17.63 ± 0.33 *(30-fold ↗)*	5.62 ± 0.41 *(2-fold ↘)*	3.14 *(60-fold ↗)*	+
Glu93Gln ox	steady-state basal	0.91 ± 0.03 (0.09 ± 0.01) [a]	15.12 ± 1.58 (6.89 ± 2.06) [a]	0.06 (0.01)	-
Glu93Gln red	steady-state	15.34 ± 0.24 *(20-fold ↗)*	10.79 ± 0.61 *(1.5-fold ↘)*	1.42 *(25-fold ↗)*	+

Oxidizing conditions, without DTT; reducing conditions, with 1 mM DTT. We estimated k_{cat}, apparent K_M for the substrate D-fructose 6-phosphate (F6P) and catalytic efficiency (k_{cat}/K_M) in a continuous spectrophotometric assay for the conversion of F6P + E4P $\rightarrow$ S7P + G3P as detailed in Methods section. In case of the oxidized, we observed a pronounced lag phase that suggested a catalytic activation under turnover conditions. We thus provide both the steady-state activities after full activation as well as basal activities at t = 0 before activation sets in. The x-*fold* change for k_{cat} and K_M for the reduced enzyme relative to the oxidized form at steady state is indicated. All measurements were carried out in triplicate and are shown as mean ± s.d.

[a] In case of catalytic activation, progress curves were fitted with eq 1 as detailed in the Methods section.

SI Table 3. Sequence conservation of NOS bridges identified in human proteins or from model organisms.

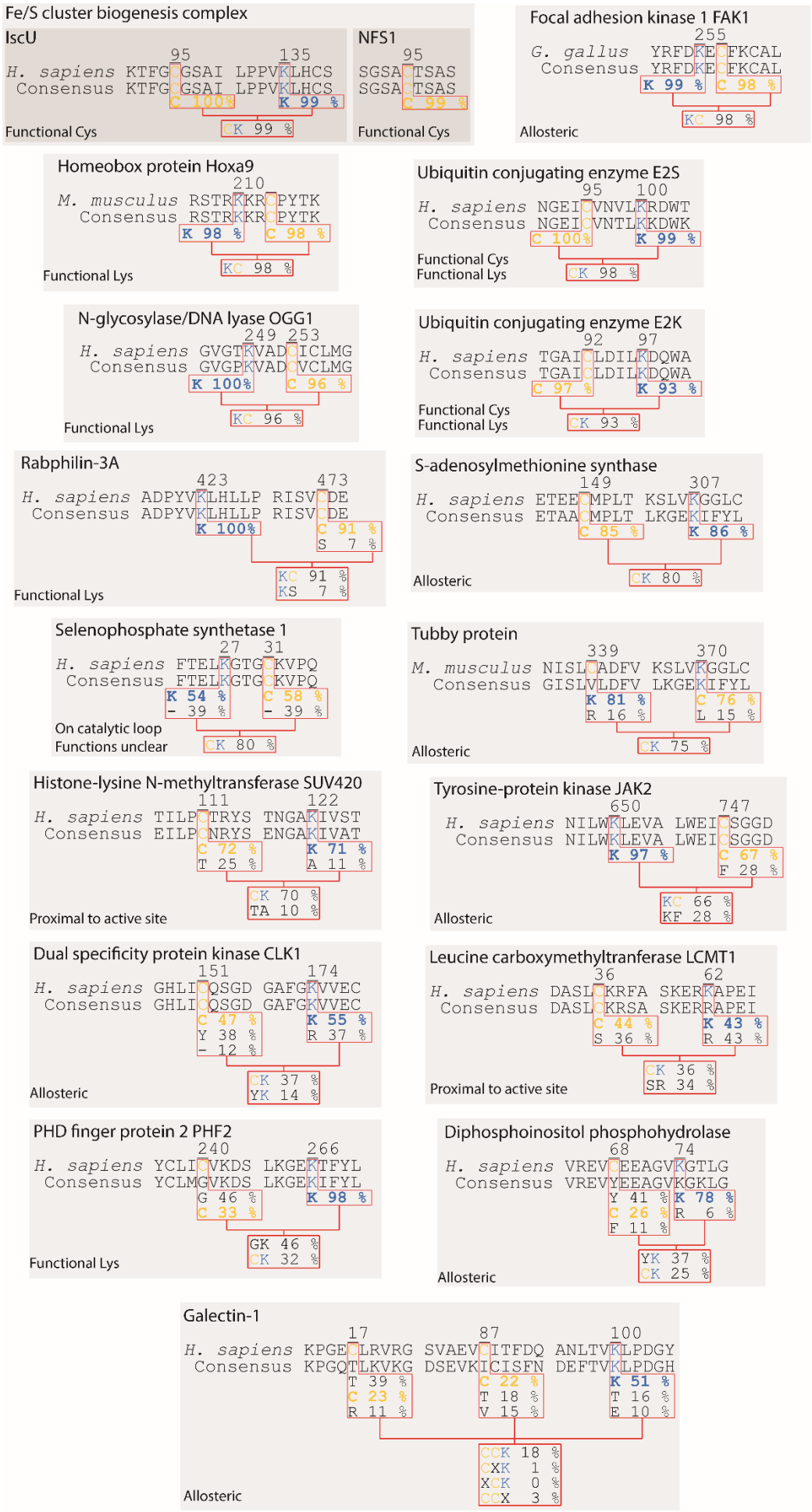

SI Table 4. Sequence conservation of NOS bridges identified in proteins from pathogens.